Collective dynamics of an active system with binary particle size

Jur de Jong

July 8, 2019

Contents

Abstract

Collective dynamics is something that can be found in nature on macro and micro scale. Since the 90s of the previous century researchers have been interested in finding a model for this group behaviour. The dynamics of a group as a whole is only determined by short-range interactions of the individuals. To better understand the working of this process, we make a model of this system with soft two-dimensional spheres with a active self-propulsion force. Furthermore there are repulsion, alignment and noise interactions, all depending exclusively on nearest neighbours. We focus on binary systems with particles of two different sizes. Migrating and rotating states are typically found in systems with homogeneous sizes. We show that these states are also found in binary systems. The migrating state has circulation of particles and this leads to segregation of the small and big particles. Small particles are more likely to be found in the tip of the group, while big particles accumulate at the tail. Active noise in the system plays a role in the degree of segregation. The lower the noise is, the more segregated the system gets in the end.

Chapter 1

Introduction

Collective behaviour of dynamic systems is found everywhere around us. One can think of a flock of birds flying south for the winter, a swarm of grasshoppers stripping the land or penguins packing together to stay warm [2, 4]. Even on the micro scale collective behaviour can be observed, for example the motion of bacterial colonies [1].

People have been wondering a long time how this collective dynamics actually works. There are some complexities, for example the lack of central regulation. Moreover, every individual does not have all information of the other individuals. And if they had, it would probably too much information to process. One individual is not even capable of influencing the group behaviour in any sense. The question that rises is then what determines the actions of the collection individuals.

With the progressing technology development and the introduction of the computer, it became possible to write a model and to do simulations. One of the first doing this were Viczek et al. [2]. Their model described a system of individuals with a orientation influenced by nearest-neighbours interactions and a noise parameter. Each individual has a self-propulsion in the direction of orientation. The system had a phase transition depending on the noise going from ordered to disordered.

Many variations have been introduced since the model of Viczek et al. [2]. The most important one for this project is proposed by Van Drongelen et al. [3]. The main differences with Viczek are that this system contains particles of finite size and the boundary conditions are not periodic any more. The finite radius of the particles is accounted for with a repulsion force, to prevent too much overlap between particles. There are also extra boundary condition added to the model, to keep the group together. Those boundary terms are only working on the outermost layer of the group, the boundary.

The simulation that were done with the model of Van Drongelen et al. [3], taught us that there are four main types of collective motion that can be performed by the system. The first phase is essentially not collective behaviour, since group breaks up in smaller groups each going their own way. The other three types of dynamics are called jammed, rotating and migrating.

These three phases are also seen in the collective behaviour of wildlife. The rotating phases corresponds to the typical doughnut shaped shoal of fish trying to confuse a predator. The migrating phase can be seen when grasshoppers are exploring the terrain looking for food And the jammed state is used by penguins to stay warm by forming a densely-packed group [2, 4]. Three examples of collective behaviour of animals are shown

in figure 1.1.

In this project we will expand the model of Van Drongelen to a system with binary particle size. The questions that we want to answer is whether a system with binary particle size still shows the same types of group behaviour? Are there differences with a system of equal particle size?

(a)

(b)

(c)

Figure 1.1: Pictures of collective behaviour found in nature. a) rotating fish confusing a predator [5] b) migrating grasshoppers looking for food [6] c) jammed penguins trying to stay warm [7].

Chapter 2

Method

This model is based on the one proposed by Van Drongelen et al. [3]. The model consists of a group of two-dimensional soft spheres. Every soft sphere is considered as a particle with a self-propulsion working in the direction of the orientation of the particle. A boundary force keeps the group together and a repulsion force prevents too much overlap between particles. Also there is torque working on the particles, that causes the orientation to change. The torque consists of three components; boundary, alignment and noise torque. This system is not stationary, because there is active self-propulsion. The resulting movement of the group can be classified in four different phases, namely rotating, migrating, jammed and a break up.

2.1 Properties

Each particle has specific dynamic properties and static properties, see table 2.1. We will explain the meaning of each property in the remainder of this chapter. The model is based on short-range interactions. The behaviour of a single particle is only influenced by neighbouring particles. The set of neighbours of particle i is called $\mathcal{N}_i$. We have a

property	symbol
position	$\vec{x}$
orientation	$\hat{\psi}$
velocity	$\vec{v}$
angular velocity	ω
force	$\vec{F}$
torque	T
boundary particle (y/n)	θ
outward angle if boundary particle	θ_{out}
Verlet list	$\mathcal{V}$
list of neighbours	$\mathcal{N}$
index (fixed)	i
radius (fixed)	a

Table 2.1: The properties of each particle.

different condition on whether particles are neighbours, because the range of radii of our particles is larger. The condition for two particles to be neighbours is that the distance between their centres is less than 1.5 times the sum of both radii. This relation is such that two particles do not necessarily need to touch to be neighbours. Furthermore this relationship is symmetric, thus if particle i has particle j as neighbour, then also particle j has particle i as neighbour.

2.2 Dynamics

Equations of motion

Each particle has a position and an orientation that are updated every time step. The movement of the particles is described as overdamped motion, thus inertia does not play a role. Then the next equations follow from the laws of mechanics [8]:

$$\vec{F}_i = \frac{32}{3}\eta a_i \vec{v}_i \equiv \alpha_i \zeta \vec{v}_i, \tag{2.1}$$

$$T_i = 4\pi\eta_R a_i^2 \omega_i \equiv \alpha_i^2 \chi \omega_i. \tag{2.2}$$

In these equations η and η_R are respectively the translational and rotational viscosity. Next we define that α_i is the normalized radius, $\alpha_i \equiv a_i/\bar{a}$. To make the equations more neat we have defined $\zeta = 32\eta/3$ and $\chi = 4\pi\eta_R$.

Force

We have to describe how the force on one particle depends on the positions of the other particles. The force exerted on a particle consists of three components, namely the self-propulsion, boundary and repulsion part,

$$\vec{F}_i = \vec{F}_{i,\mathrm{self-propulsion}} + \vec{F}_{i,\mathrm{boundary}} + \vec{F}_{i,\mathrm{repulsion}}. \tag{2.3}$$

The self-propulsion force depends on a parameter F_{self} and works in the direction of the orientation $\hat{\psi}_i$ of the particle,

$$\vec{F}_{i,\mathrm{self-propulsion}} = F_{\mathrm{self}} \hat{\psi}_i. \tag{2.4}$$

The boundary force causes the particles to stay together as a group. The force is only active if the particle is at the boundary. To determine whether a particle is at the boundary, the next steps are followed; check the surroundings of a particle i in anti-clockwise direction. If there is a gap without neighbours $\theta_{\mathrm{out},i}$ of more than π, then the particle is considered to be a boundary particle. The boundary force consists of a parameter F_{in} multiplied by the difference of θ_{out} and π. The boundary force works in the direction of the orientation.

$$\vec{F}_{i,\mathrm{boundary}} = \begin{cases} 0 & \text{if } \theta_{\mathrm{out}} < \pi \\ F_{\mathrm{in}}(\theta_{\mathrm{out}} - \pi)\hat{\psi}_i & \text{if } \theta_{\mathrm{out}} \geq \pi \end{cases} \tag{2.5}$$

The repulsion force is there to prevent the particles from overlapping to much. It

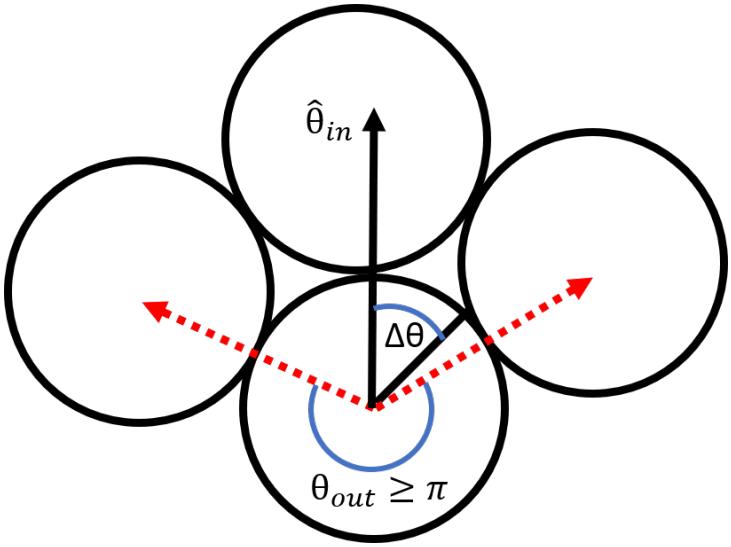

Figure 2.1: An illustration of how θ_{out}, $\hat{\theta}_{\text{in}}$ and $\Delta\theta$ are defined. $\theta_{\text{out},i}$ is the largest gap between neighbours, $\hat{\theta_{\text{in}}}$ is the exterior bisector of θ_{out} and $\Delta\theta$ is the difference between $\hat{\psi}_i$ and $\hat{\theta}_{\text{in}}$.

depends on the overlap between two particles times a spring constant k. Here $\vec{d_{ij}}$ points in the direction of the difference between positions of particles i and j. Further $|\vec{d_{ij}}|$ is proportional to the surface of overlapping.

$$\vec{F}_{i,\text{boundary}} = -k \sum_{j \in \mathcal{N}_i} \vec{d_{ij}} \tag{2.6}$$

Torque

The equation of the torque also contains three main components; the boundary, the noise and the alignment term,

$$T_i = T_{i,\text{boundary}} + T_{i,\text{noise}} + T_{i,\text{alignment}}. \tag{2.7}$$

The boundary torque makes the orientation of the boundary particles point to the bulk of the group. It only has a value other than 0 when the particle is a boundary particle. Here $\hat{\theta}_{\text{in}}$ is the exterior bisector of θ_{out}, such that $\hat{\theta}_{\text{in}}$ is pointing to the bulk of the group, see figure 2.1. The difference between the orientation $\hat{\psi}_i$ and $\hat{\theta}_{\text{in}}$ is called $\Delta\theta$. The torque scales linearly with $\Delta\theta$. Furthermore, it is scaled by the parameter T_{in}.

$$T_{i,\text{boundary}} = \begin{cases} 0 & \text{if } \theta_{\text{out}} \leq \pi \\ T_{\text{in}} \Delta\theta_i & \text{if } \theta_{\text{out}} > \pi \end{cases} \tag{2.8}$$

The noise component in the torque represents the random processes. A single particle in this model would perform a random walk, because of the presence of this noise term. The noise consists of a scaling parameter T_{noise} and a random variable ξ which is drawn every time step from an uniform distribution from -1 to 1,

$$T_{i,\text{noise}} = T_{\text{noise}} \xi_i. \tag{2.9}$$

The alignment term makes the particles willing to have the same orientation as there neighbours. It depends on a scaling parameter T_{align} and the sum of the mismatch in orientation between the neighbours and the particle itself. $\Delta\psi_{ij}$ scales proportional to the mismatch in orientation,

$$T_{i,\text{alignment}} = T_{\text{align}} \sum_{j \in \mathcal{N}_i} \Delta\psi_{ij}. \tag{2.10}$$

2.3 Scaling parameters

We define the characteristic time $\tau = \zeta/k$ for two overlapping particles to separate due to the repulsion force. The other time scales are determined in appendix A and presented in table 2.2, only the self-propulsion force has no time scale because it is an active force [3]. We define dimensionless scaling parameter that we use for influencing the group dynamics. For interaction X we define the dimensionless scaling parameter $\lambda_X = \tau/\tau_X$ [3]. In the last column of table 2.2 we have rewritten the dimensionless parameter to the characteristic parameter, such that we can fill it in equations 2.4 and 2.7.

The most interesting phase to observe is the migrating state. The results from Van Drongelen et al. [3] can be used to obtain this state. The values of $\lambda_{F_{in}}$ and $\lambda_{T_{in}}$ are chosen to be respectively 0.3 and 3.0. The value of those parameters does not change the behaviour of the group significantly [3]. Varying λ_a and λ_s change the type of collective motion.

Interaction	Time scale	Dimensionless scaling parameter	Characteristic parameter
Repulsion	$\tau = \zeta/k$		$k = \zeta/\tau$
Alignment	$\tau_{\text{align}} = \chi/T_{\text{align}}$	$\lambda_a = \zeta T_{\text{align}}/k\chi$	$T_{\text{align}} = \lambda_a k\chi/\zeta$
Noise	$\tau_{\text{noise}} = 2\chi^2/T^2_{\text{noise}}\Delta t$	$\lambda_n = \zeta T^2_{\text{noise}}\Delta t/2k\chi^2$	$T_{\text{noise}} = \chi\sqrt{2\lambda_n k/\zeta\Delta t}$
Inward force	$\tau_{\text{F}_{\text{in}}} = \zeta\bar{a}/F_{\text{in}}$	$\lambda_{\text{F}_{\text{in}}} = F_{\text{in}}/k\bar{a}$	$F_{\text{in}} = \lambda_{F_{in}} k\bar{a}$
Inward torque	$\tau_{\text{in}} = \chi/T_{\text{in}}$	$\lambda_{T_{in}} = \zeta T_{\text{in}}/k\chi$	$T_{\text{in}} = \lambda_{T_{in}} k\chi/\zeta$
Self propulsion	–	$\lambda_s = F_{\text{self}}/k\bar{a}$	$F_{\text{self}} = \lambda_s k\bar{a}$

Table 2.2: An overview of the time scale, scaling parameter and characteristic parameter per interaction. The dimensionless parameter for interaction X is defined as $\lambda_X = \tau/\tau_X$. The characteristic parameter is a rewritten form of the dimensionless parameter such that it can be used for the calculations.

2.4 Initiation

Before the simulation can start, the system has to be initiated. The properties of each particle get an initial value. First, there will be N particles created in the system. Every particle i will get a radius a_i, a position x_i and an orientation $\hat{\psi}_i$. The position will be such that the particles will be placed on a grid of 10 particles wide. The orientation will be upwards with a deviation between $-\pi/4$ and $\pi/4$ drawn from a uniform distribution.

When the system is initiated, there will be particles with a considerable amount of overlap with the other particles. To solve this, the system will get some time to relax. This means all the force and torque components are present, except for the self-propulsion force. The system of particles will expand until there is almost no overlap between the particles. Now, the self-propulsion is switched on. When the difference in radius between the particles increases, the time to relax should also increase, because there is more initial overlap.

Each time step consists of two main steps. First for the given positions and orientations of the particles, the force and torque are determined. Then the velocity and angular velocity are updated. The second step is to update the position and orientation for every particle. Now we begin a new cycle by determining the force and torque for the new situation.

2.5 Simulation

When the initiation has gone right, the simulation can start. For each time step, the force and torque can be determined for every particle with equations (2.4) and (2.7). We integrate the equations of motion (2.1, 2.2) with the Euler forward method. This gives equations (2.11) and (2.12), notice that for equation (2.12) $\hat{\psi}$ is first transformed in radians, such that ψ is not a vector any more. The time step Δt is chosen to be 0.1τ, such that

$$\vec{x_i}(t + \Delta t) = \vec{x_i}(t) + \vec{v_i}(t)\Delta t = \vec{x_i}(t) + \frac{\vec{F_i}(t)}{\alpha_i \zeta}\Delta t, \tag{2.11}$$

$$\psi_i(t + \Delta t) = \psi_i(t) + \omega_i(t)\Delta t = \psi_i(t) + \frac{T_i}{\alpha_i^2 \chi}\Delta t. \tag{2.12}$$

Verlet list

For updating the force and the torque, the neighbours of every particle need to be determined every time step. That takes a lot of computation time. To reduce the computation time, the implementation of the model uses Verlet lists, inspired by McCusker et al. [9] and invented by Verlet et al. [10]. This is a list of potential neighbours of a particle. This list is determined by considering which particles are within a certain skin radius, r_s. The skin radius has to be considerably larger than the radius for being neighbours, r_n. The advantage of using a Verlet list is that not every time step every particle has to check all other particles if they are neighbours. Only the particles within the Verlet list are potential neighbours. Figure 2.2 shows an illustration of a Verlet list.

When there is the possibility for one particle to be moved from outside the skin radius to within the neighbour radius, then the Verlet list should be updated. To check this, one should keep track of the maximum change in distance between two particles. The two maximum absolute displacements are saved, because this is the maximum change in distance between two particles. Once the sum of maximum displacements exceeds the difference between the skin radius and the neighbour radius, the Verlet lists of all particles are updated.

If the skin radius r_s is chosen small, the Verlet list of a particle contains few potential neighbours. However the Verlet lists need to be updated very frequently. So r_s must be

chosen such that there is a good balance between those two effects. The biggest r_n is attained when we consider two big particles. For two particles of radius 2, $r_n = 1.5(2+2)$ thus $r_s > 6$. We tried different values of r_s and this found us that the fastest simulations are achieved when $r_s = 7$.

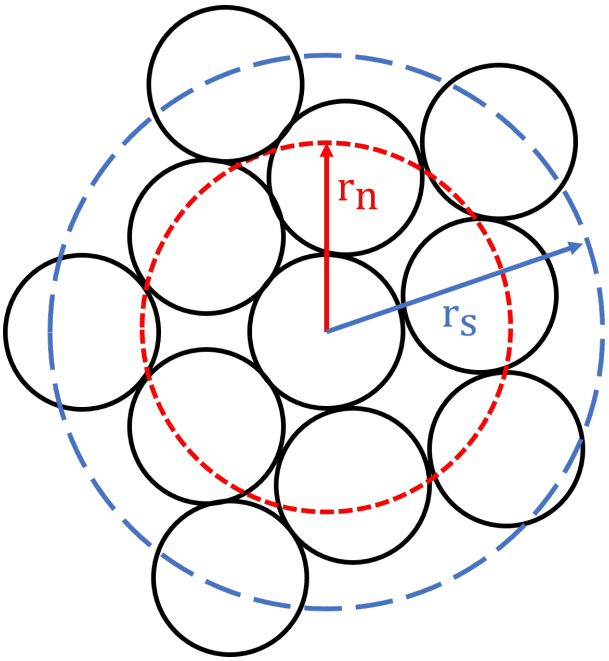

Figure 2.2: Illustration of the calculations done when using a Verlet list. The red arrow describes the neighbour radius. The blue arrow describes the skin radius that defines the Verlet list.

2.6 Size correlation function

To get a better understanding of the separation between particles of different size, we use the size correlation function

$$\gamma = \frac{s_{ab}}{\sqrt{s_{aa}s_{bb}}}. \tag{2.13}$$

The definition of γ makes use of s_{aa}, s_{bb} and s_{ab} which are defined following equations (2.14a),(2.14b) and (2.14c). We define N as the total amount of particles in the system. We remember that a_i is the radius of a particle, such that $\bar{a}$ is the average radius of all particles. Then b_i is the average radius of all neighbours of particle i, and $\bar{b}$ is the average of all b_i's. This gives the equations:

$$s_{aa} = \frac{1}{N}\sum_i (a_i - \bar{a})^2, \tag{2.14a}$$

$$s_{bb} = \frac{1}{N}\sum_i (b_i - \bar{b})^2, \tag{2.14b}$$

$$s_{ab} = \frac{1}{N}\sum_i (a_i - \bar{a})(b_i - \bar{b}). \tag{2.14c}$$

When the group is initiated, the location of the small and big particles is completely random. Thus the expectation is that γ should be around zero at the start of the simulation. As the smaller particles begin to separate from the bigger particles, γ should increase towards 1. When γ is 1, the group is totally separated. This is not likely to occur, since there should always be a separation interface. To reduce the running time γ is saved once every 50 time steps.

Maximum size correlation function

When the groups have not separated, there is a transition interface between the group of big and small particles. This makes the size correlation function less than 1 and is practically 1 for a system initialized in a random configuration. The estimation is described in appendix B.

Chapter 3

Results

3.1 Particles with the same radii

All simulations are done with 200 particles, to keep the running time reasonable. As in Van Drongelen et al. [3], the parameters $\lambda_{\mathrm{F_{in}}} = 0.3$ and $\lambda_{\mathrm{T_{in}}} = 3$ are kept constant for all simulations. In sections 3.1 and 3.2 $\lambda_n = 0.03$, but in section 3.4 λ_n is varied.

The first simulations are done with all radii drawn from a single Gaussian distribution with $\mu = 1$ and $\sigma = 0.1$, to check whether the results are the same as [3]. Two snapshots of these simulations are shown in figure 3.1. The blue particle are 'normal' particles and the red particles are boundary particles. The group is able to move on a infinite 2 dimensional plane. Subfigure (a) is a snapshot of a simulation in the migrating phase, with $\lambda_s = 0.06$ and $\lambda_a = 0.3$. This group contains one defect towards which all particles are orientated. The net movement of the group will be in the direction of the defect. Subfigure (b) is a screen shot of a simulation in the rotation phase, with $\lambda_s = 0.08$ and $\lambda_a = 0.1$. This group has no defect, because there is a hole in the middle, so there is no defect necessary. The rotating phase has very little net movement, because almost all individual movement cancel each other.

Something noticeable is that there is circulation within the migrating state, illustrated in figure 3.2. We take a closer look at a particle near the defect of the group. The orientation of almost all particles is towards this particle, so their self-propulsion cause a high pressure on this particle. The particle will be pushed towards the very front tip of the group. The boundary torque turns the orientation inwards such that the orientation is in the opposite direction of the group movement. The particle will move via the boundary to the tail of the group. Once at the tail the pressure in the bulk of the group is low. The particle will move inside the bulk of the group towards the defect. This process is illustrated in figure 3.2.

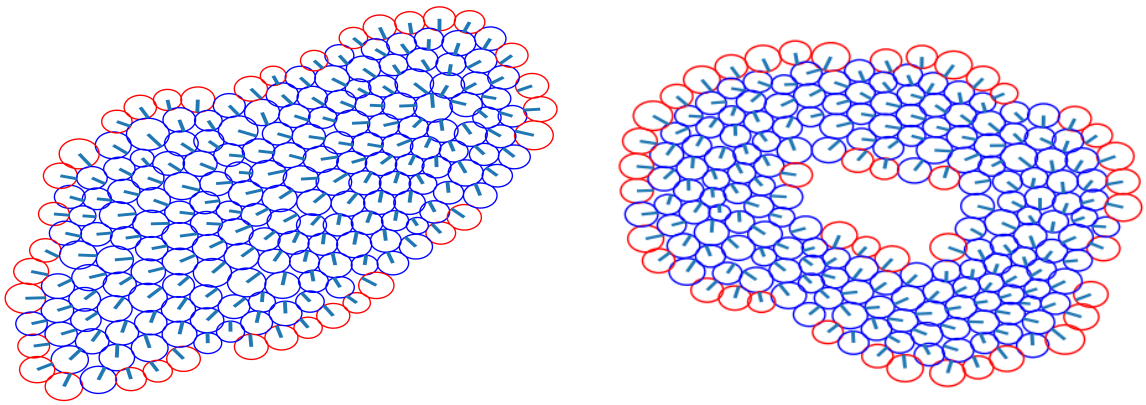

(a) (b)

Figure 3.1: Snapshots of simulations with 200 particles with radii drawn from a single Gaussian distribution. (a) The migrating state with $\lambda_s = 0.06$ and $\lambda_a = 0.3$ (b) The rotating state with $\lambda_s = 0.08$ and $\lambda_a = 0.1$.

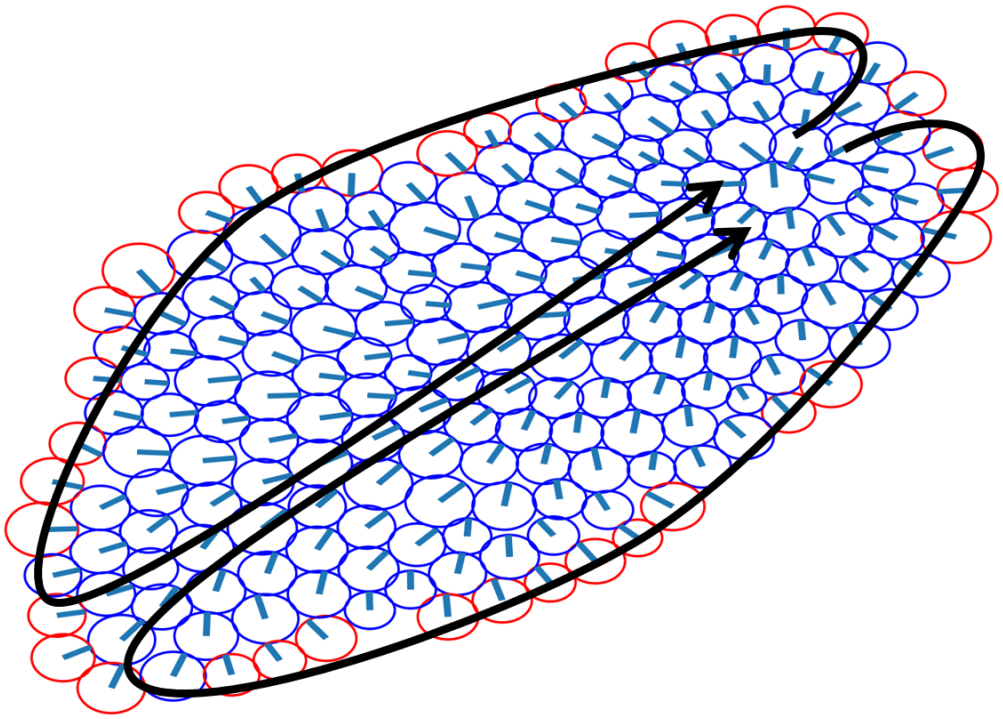

Figure 3.2: An illustration of the circulation within a migrating group.

3.2 Particles with different radii

The model is changed to a binary system with particle of significant different size. Every particle has an equal chance of having radius 1 or 2, such that there are approximately as many big as small particles. Figure 3.3(a) and (b) show snapshots of the simulations with the same parameters as in figure 3.1. Again, we see that the two different phases are present, namely the migrating and rotating state. Also there is still circulation of particles in both phases, indicated with black arrows in figure 3.3. If we take a closer look at the migrating state, we see that a lot of big particles are at the tail of the group, while the small particles are more at the tip of the group. If we look at the rotating state, we see that the inner and outer boundary contain only big particles. The inner and outer rings of particles in the rotating state show little movement, while inside the ring there is circulation of mainly small particles and some big particles. Furthermore, the big particles at the tail are showing few rearrangements, because there equal size cause them to close pack. To prevent this phenomenon of crystallization, the model is changed to a system where the radii are drawn from $N(1, 0.01)$ and $N(2, 0.04)$, such that a group

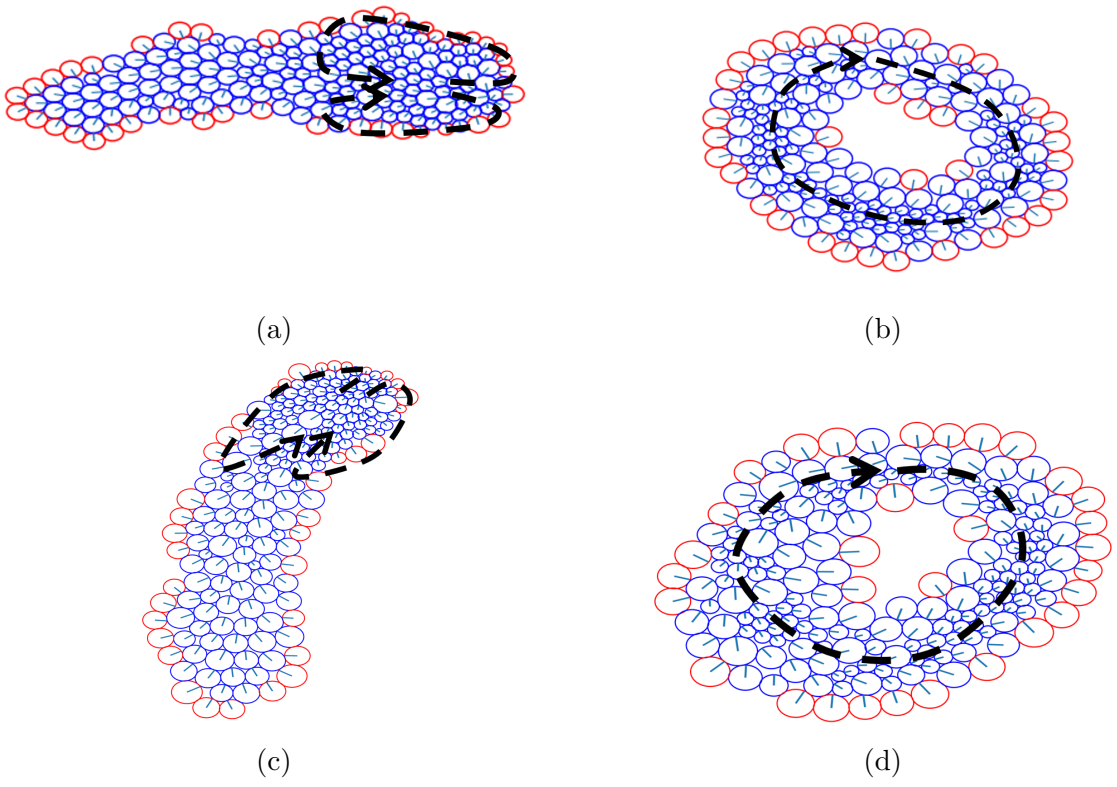

Figure 3.3: Snapshots of simulations with 200 particles. The way of circulation is indicated with black arrows. (a) and (b) have radii of exactly 1 and 2. (c) and (d) have radii drawn from $N(1, 0.01)$ and $N(2, 0.04)$. (a) and (c) $\lambda_s = 0.06$ and $\lambda_a = 0.3$. This gives the migrating state. (b) and (d) $\lambda_s = 0.08$ and $\lambda_a = 0.1$. These values give the typical rotating state.

of exclusively big particles is a scaled version of a group of exclusively small particles. If we look at the snapshots, c) and d) of figure 3.3, we can see that this change does not influence the behaviour of the group.

One could ask whether the segregation of different particles also happens when the system is not binary, but instead a continuum of different radii. This is obtained by taking the radii from a single Gaussian distribution with increased σ. In figure 3.4a) we see a snapshot of a simulation with $\sigma = 0.2$. It can be seen that there is a substantial difference between radii. Again, there is some visible segregation between the smaller and bigger particles. Figure 3.4b) shows the progression of the correlation parameter γ for this single simulation. This also indicates that there is segregation, however it seems to grow slower in time and is not growing beyond 0.6.

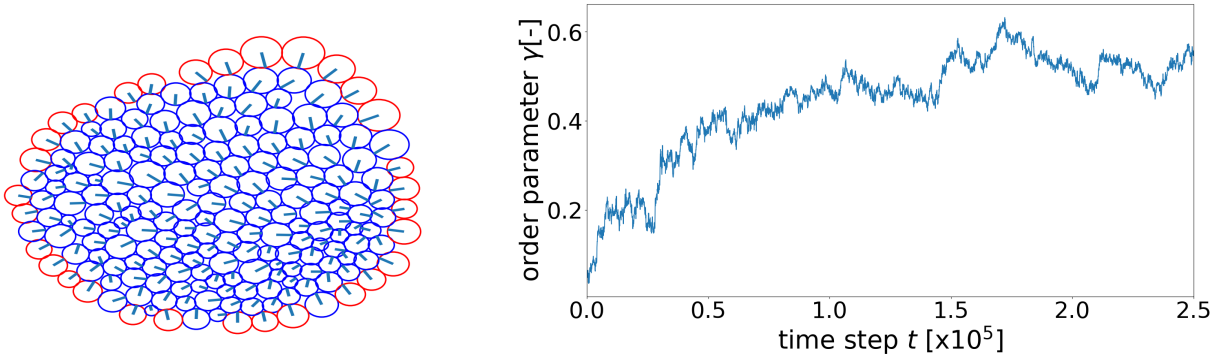

(a) (b)

Figure 3.4: The results of a simulation with radii drawn from $N(1, 0.2)$. a) A snapshot of the simulation. b) The evolution of γ as time proceeds. NOTE: I'm still working on getting the axis fonts bigger, but have not find out yet how to do that.

3.3 Segregation

We see that there is segregation of the small and big particles in the migrating phase. The big particles are found at the tail of the group and the small particles in the tip. Eventually, the group splits up in one group of mainly small particles and one group of mainly big particles. The process of segregation looks like the Brazil Nut Effect [11, 12]: when you shake a bowl with small and big nuts, the big nuts rise to the top. The Brazil nut effect can be explained as follows. When you shake the bowl, the system will be disordered and the nuts are lifted slightly. There emerge holes between the nuts. The chance that there emerges a hole such that a small nut can fit underneath the big nut is more likely than the other way around [11]. Therefore the chance that a small nut is moving down is larger than that of a big nut moving down. We use the explanation of the Brazil nut effect to describe the process of segregation in the binary model of moving particles.

The circulation of particles moving from the bulk to the tip and via the boundary to the back is still present. The particles are of different sizes, so there is no crystallization. Due to the movement of the particles and the noise, small holes between particles will emerge and disappear. This makes that the particles at the tail can move back in to the bulk of the group. The chance of emerging a small hole such that a small particle can move inwards, is likely. But it is not likely that there emerges a hole where a big particle fits in. The consequence is that the big particles accumulate at the tail, while the small particles can still circulate through the group.

After this process has been going on for a while, there is a long tail of almost only big particles. At most a few small particle are stuck in the tail of big particles and they cannot move out because there is not much circulation inside the tail. Our definition of the self-propulsion makes that a bigger radius leads to a lower velocity when the forces are approximately equal. This is also an effect why the big particles are getting behind, while the small particles go to the tip. When the group is still mixed, the boundary force keeps the group together. The small particles take the big particles with them. When there is more segregation, the big particles are gathered in the tail and they lack speed to keep up with the small particles. This is a minor effect, but when there is almost full segregation, this effect becomes significant. The group of big and small particles will split up in one group of almost exclusively big particles and one faster moving group of small particles.

3.4 Noise

To find out whether the rate of segregation depends on the noise, simulations are done for different values of the noise parameter λ_n. There are 5 simulations of 500.000 time steps done for every different value of λ_n. The value of the size correlation function is saved every 50th time step. The results are shown in figure 3.5(a). We will fit a exponential function through the data points of the form

$$\gamma = \gamma_0 - \gamma' e^{-t/\tau}. \tag{3.1}$$

Furthermore, the size correlation function seems to equilibrate at a higher value for lower noise. The reason for this is that a system with advanced segregation has little circulation.

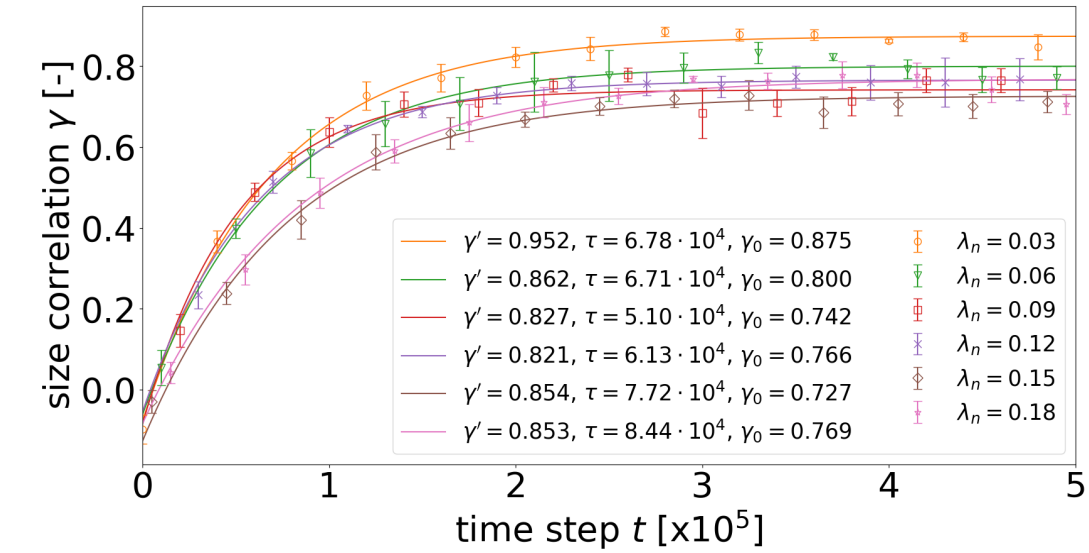

(a)

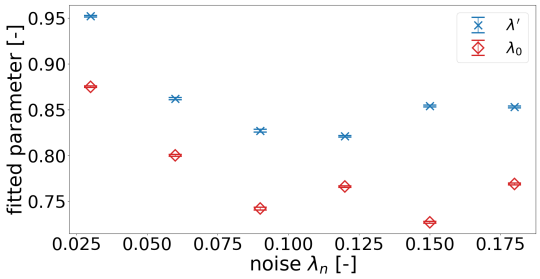

(b)

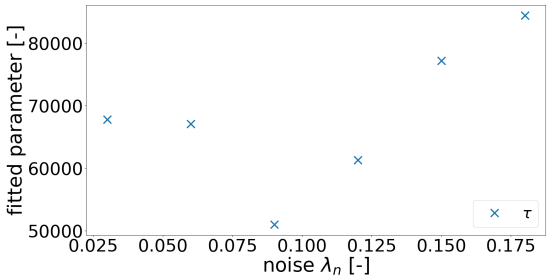

(c)

Figure 3.5: The results of simulations with 200 particle for different values of λ_n. (a) The evolution of the size correlation function γ for different values of λ_n. The fitted curves are of the form $\gamma = \gamma_0 - \gamma' e^{-t/\tau}$. All curves get a constant value as time proceeds. (b) Plot of the fitted parameters λ' and λ_0 with the standard deviation of the fit. (c) Plot of the fitted τ without the standard deviation, because it is of the order 10^{-3}, so it is not visible.

There is not enough circulation to segregate further. For $\lambda_n = 0.03$ the fitted curve tells us that the size correlation value will converge to $\gamma = 0.875$. That is reasonably lower than 1 as we approximated in appendix B.

There seems to be a gap in the rising part of the order parameter around time step 100.000 between $\lambda_n \leq 0.12$ and $\lambda_n \geq 0.15$, but further examination shows that we have not done enough simulations yet. More simulations are done for $\lambda_n = 0.12$ and $\lambda_n = 0.15$. We run 20 more simulations for these values of λ_n. The results are shown in figure 3.6(a). There is still a gap, but it is within the error bars.

To reduce the influence of the starting distribution, we choose to do multiple simulations with the same starting configuration. The standard beginning distribution is chosen such that the order parameter is close to zero when the simulation starts. The results are shown in figure 3.6(b). The decay of γ in for $\lambda_n = 0.12$ is due to several simulations getting into the rotating state. Then the system gets more mixed, such that γ becomes lower. Both figure 3.6(a) and (b) show no considerable difference between simulations with $\lambda_n = 0.12$ and $\lambda_n = 0.15$.

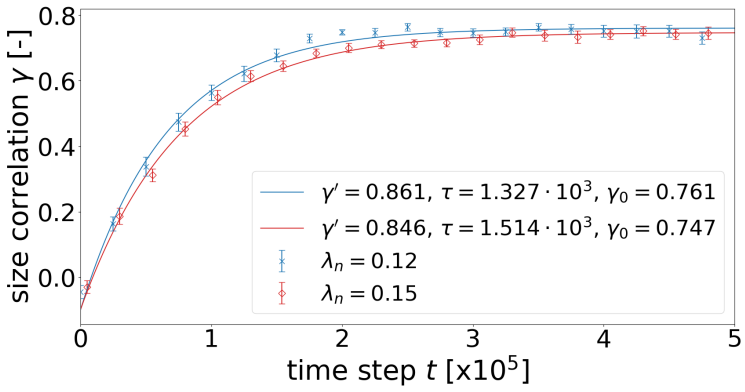

(a)

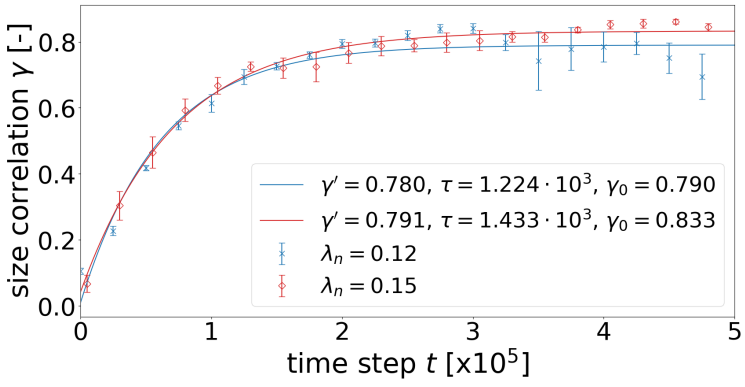

(b)

Figure 3.6: The evolution of γ for $\lambda_n = 0.12$ and $\lambda_n = 0.15$. a) The average result over 25 simulations. b) The average result of 5 simulation all with the same initial configuration.

Chapter 4

Conclusion

One of the research questions was whether a system with binary particle size would perform the same types of collective behaviour as system with equal particle size. We conclude that a binary system with particles of radii 1 and 2 can be in the migrating and rotating state. The migrating state is found for $\lambda_s = 0.06$ and $\lambda_a = 0.3$ and the rotating state is found for$\lambda_s = 0.08$ and $\lambda_a = 0.1$. These values are the same as for a system with equal particle size. Also there is circulation of particles within a group in the migrating state. Particles are moving from the front tip via the boundary to the tail and through the bulk back to the tip. Smaller particles are more likely to re-enter the bulk, while big particles are accumulating at the tail. This causes segregation of small and big particles as time proceeds, which is an additional effect compared to a system with equal particle size.

The noise parameter λ_n influences the way the system segregates. The lower λ_n, the higher the value of γ finally becomes, so the higher the order of segregation. The lowest value of λ_n tested in this project, gives the final value of $\gamma = 0.875$. This is a reasonable difference with the theoretical optimal value. The reason that γ does not grow further is that when the system is in an advanced stadium of segregation, there is not enough circulation to segregate further.

Appendix A

Determine characteristic times

We want to determine a time scale τ_X for interaction X. We do this by solving the differential equation of interaction X. We define that the time scale for two overlapping particle to separate is $\tau = \zeta/k$. If we look at the differential equation for one particle to align with one other particle

$$\chi\dot{\theta} = T_{\text{align}}\theta. \tag{A.1}$$

The solution to this equation is

$$\theta = \theta_0 e^{tT_{\text{align}}/\chi} = \theta_0 e^{t/\tau_{\text{align}}}. \tag{A.2}$$

So we see that $\tau_{\text{align}} = \chi/T_{\text{align}}$. Then for the noise we get the stochastic differential equation

$$\chi\dot{\theta} = T_{\text{noise}}\xi. \tag{A.3}$$

The solution is [13]

$$\theta = \theta_0 e^{-\frac{1}{2}(T_{\text{noise}}/\chi)^2\Delta t} = \theta_0 e^{-1/\tau_{\text{noise}}}. \tag{A.4}$$

Thus $\tau_{\text{noise}} = 2\chi^2/T_{\text{noise}}^2\Delta t$. If we look at the boundary force, we consider two particles with their centre on the x-axis and in between one particle slightly above the x-axis, see figure A.1. The boundary force scales with $\theta_{\text{out}} - \pi$. We want to determine for the middle particle the angle between the horizontal and the vector pointing to the left particle. The vertical distance is x and the horizontal distance is approximately $2\bar{a}$, so the angle is $\arctan(x/2\bar{a})$. Also for the angle between the horizontal and the vector pointing to the right particle is $\arctan(x/2\bar{a})$. Then $\theta_{\text{out}} - \pi = 2\arctan(x/2\bar{a}) \approx x/\bar{a}$. That results in the equation for the inward force

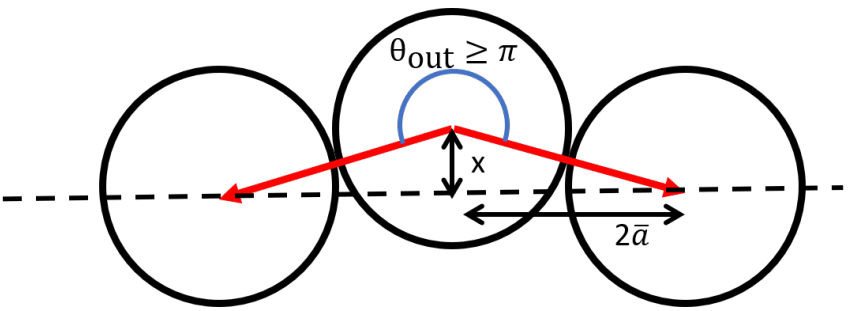

Figure A.1: An illustration of how the time scale for the boundary force is determined.

$$\zeta \dot{x} = F_{\text{in}} x/\bar{a}, \tag{A.5}$$

with the solution

$$x = x_0 e^{F_{\text{in}}/\bar{a}\zeta} = x_0 e^{t/\tau_{\text{F}_{\text{in}}}}. \tag{A.6}$$

We conclude that $\tau_{\text{F}_{\text{in}}} = \zeta \bar{a}/F_{\text{in}}$. For the boundary torque we consider one particle at the boundary not orientated towards the bulk. The differential equation is

$$\chi \dot{\theta} = T_{\text{in}} \theta \tag{A.7}$$

We repeat the method of previous cases and we find that $\tau_{\text{T}_{\text{in}}} = \chi/T_{\text{in}}$.

Appendix B

Estimate the maximum size correlation function

We want to have a reasonable approximation of the maximum value of the size correlation called $\gamma_{\max}$, without the particles being separated in completely isolated groups. Considering a binary system with two different radii, we define p as the fraction of small particles of the total amount of particles N. For our model the average value of $p = 0.5$. So $1 - p$ is the fraction of big particles. Next we define r to be the ratio between big and small particles. For convenience we scale the radius of the small particles to $a_{\text{small}} = 1$,

$$r = \frac{a_{\text{big}}}{a_{\text{small}}} = a_{\text{big}}. \tag{B.1}$$

The average radius of the particles $\bar{a}$ is now

$$\bar{a} = \frac{1}{N}\sum_i a_i = \frac{1}{N}(1pN + r(1-p)N) = p + r - rp. \tag{B.2}$$

We can now calculate s_{aa},

$$\begin{aligned} s_{aa} &= \frac{1}{N}\sum (a_i - \bar{a})^2 \\ &= \frac{1}{N}(Np(1-\bar{a})^2 + N(p-1)(r-\bar{a})^2) \\ &= p(1-p-r+rp)^2 + (p-1)(r-p-r+rp)^2 \\ &= p(p-1)\left[(p-1)(r-1)^2 - p(1+r)^2\right]. \end{aligned} \tag{B.3}$$

Next we will consider b_i, that is the average radius of the neighbours of one particle. Suppose the group if completely segregated, except for a transition interface, where the groups of small and big particles are touching. Then we define the following parameters:

- $n_{\text{small,i}}$ is the amount of small particles at the transition interface
- $n_{\text{big,i}}$ is the amount of big particles at the transition interface
- $n_{\text{small,b}}$ is the amount of small particles in the bulk
- $n_{\text{big,b}}$ is the amount of big particles in the bulk

- c_{small} is the fraction of small neighbours of a small particle at the transition interface.
- c_{big} is the fraction of small neighbours of a big particle at the transition interface.

Note that small particles in the bulk of the group are surrounded exclusively by small particles, but small particles at the transition interface are partly surrounded by small particles and partly by big particles. The same holds for big particles.

We know that the total amount of small particles is Np and big particles is $N(1-p)$, thus then

$$Np = n_{\text{small,b}} + n_{\text{small,i}}, \tag{B.4}$$
$$N(1-p) = n_{\text{big,b}} \quad + n_{\text{big,i}}. \tag{B.5}$$

So when $n_{\text{small,i}}$ and $n_{\text{big,i}}$ are set, the amount of particles that are not at the interface, $n_{\text{small,b}}$ and $n_{\text{big,b}}$, are automatically fixed. The interface for small and big particles have about the same length. Taking into account the smaller radius, we estimate that $n_{\text{small,i}}$ is r times $n_{\text{big,i}}$. The particles not at the interface are exclusively surrounded by particles of the same size. This gives the values $b_{\text{small,b}} = 1$ and $b_{\text{big,b}} = r$. We need to give a closer look at the particle that actually are at the transition interface. There are $b_{\text{small,i}}$ small particles at the interface and the average radius of their neighbours is calculated as

$$b_{\text{small,i}} = 1 \cdot c_{\text{small}} + r \cdot (1 - c_{\text{small}})\,. \tag{B.6}$$

And for the big particles we get

$$b_{\text{big,i}} = 1 \cdot c_{\text{big}} + r \cdot (1 - c_{\text{big}})\,. \tag{B.7}$$

We get for the average radius of the neighbours

$$\begin{aligned} \bar{b} &= \frac{1}{N} \sum_i b_i \\ &= \frac{1}{N} \left[n_{\text{small,b}} b_{\text{small,b}} + n_{\text{small,i}} b_{\text{small,i}} + n_{\text{big,b}} b_{\text{big,b}} + n_{\text{big,i}} b_{\text{big,i}} \right]. \end{aligned} \tag{B.8}$$

Now we can determine s_{bb} and s_{ab},

$$\begin{aligned} s_{bb} &= \frac{1}{N} \sum_i (b_i - \bar{b})^2 \\ &= \frac{1}{N} \Big[n_{\text{small,b}} \left(b_{\text{small,b}} - \bar{b} \right)^2 + n_{\text{small,i}} \left(b_{\text{small,i}} - \bar{b} \right)^2 + \\ &\qquad n_{\text{big,b}} \left(b_{\text{big,b}} - \bar{b} \right)^2 + n_{\text{big,i}} \left(b_{\text{big,i}} - \bar{b} \right)^2 \Big], \end{aligned} \tag{B.9}$$

$$\begin{aligned} s_{ab} &= \frac{1}{N} \sum_i (a_i - \bar{a})(b_i - \bar{b}) \\ &= \frac{1}{N} \Big[(1 - \bar{a}) \Big[n_{\text{small,b}} \left(b_{\text{small,b}} - \bar{b} \right) + n_{\text{small,i}} \left(b_{\text{small,i}} - \bar{b} \right) \Big] + \\ &\qquad (r - \bar{a}) \Big[n_{\text{big,b}} \left(b_{\text{big,b}} - \bar{b} \right) + n_{\text{big,i}} \left(b_{\text{big,i}} - \bar{b} \right) \Big] \Big]. \end{aligned} \tag{B.10}$$

And finally we have

$$\gamma = \frac{s_{ab}}{\sqrt{s_{aa}s_{bb}}}. \tag{B.11}$$

To determine the optimal value of γ of a fully segregated system, we need to define values for c_{small}, c_{big} and $n_{\text{big,i}}$. To do this, we run a simulation with all particles with radius 2 in the lower half of the initial grid and all particles with radius 1 in the upper half. We let this simulation run for 10.000 time steps, so that it can find a stable configuration. A screenshot of this simulation is shown in figure B.1a. There are many

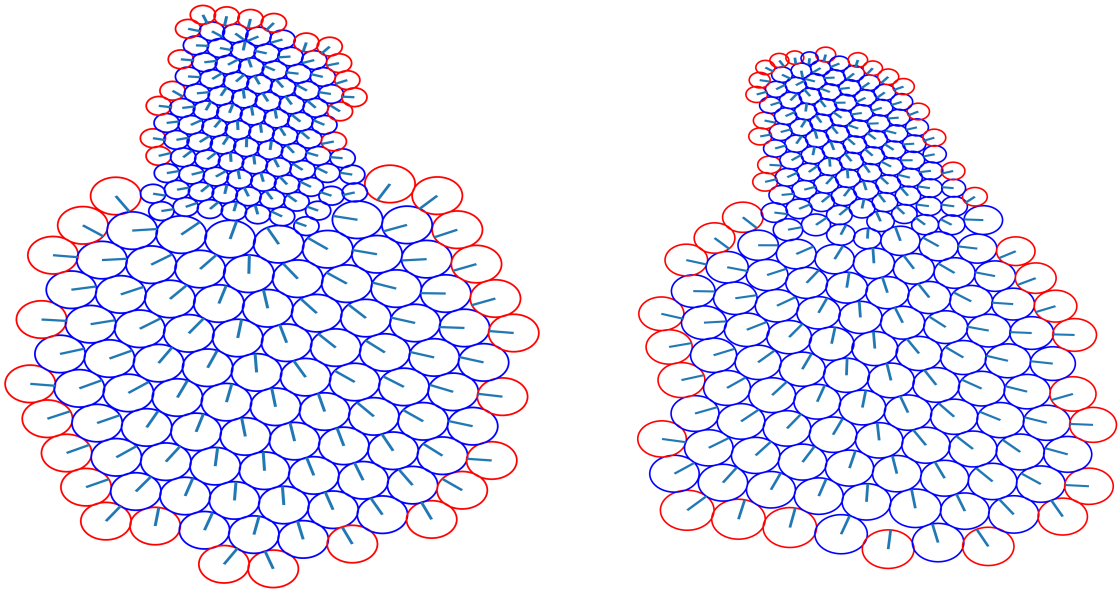

(a) (b)

Figure B.1: Snapshots of optimally segregated systems. a) This systems consists particle with radii of exactly 1 or 2. b) This systems contains particles with radii drawn from $N(1, 0.01)$ and $N(2, 0.04)$.

configurations where the system is completely segregated, but the one in figure B.1(a) gives us a good indication of the desired parameters. This situation tells us that $n_{\text{big,i}} = 8$ and $n_{\text{small,i}} = 12$, so the estimate of $n_{\text{small,i}} \approx r n_{\text{big,i}}$ not very accurate. If we look closely at the interface of figure B.1(a), we can determine the other parameters, namely $c_{\text{small}} = 0.71$ and $c_{\text{big}} = 0.35$. Using these values, we can calculate that $\gamma_{\max} = 0.97$.

In this project we are working with particle drawn for a Gaussian distribution. We first create 200 particles with a chance of 0.5 that the radius is drawn from $N(1, 0.01)$ and a chance of 0.5 that the radius is drawn from $N(2, 0.04)$. Then we sort the particles from big to small. The biggest particles are placed at the bottom of the grid while the smallest particles are at the top. We let the simulation do 10.000 time steps to find a stable configuration. A snapshot of this simulation is shown in figure B.1(b). The value that γ has for this distribution is practically 1.

Bibliography

[1] H.-P. Zhang, A. Beer, E.-L. Florin, and H. L. Swinney, Proceedings of the National Academy of Sciences **107**, 13626 (2010).

[2] T. Vicsek, A. Czirók, E. Ben-Jacob, I. Cohen, and O. Shochet, Physical review letters **75**, 1226 (1995).

[3] R. van Drongelen, A. Pal, C. P. Goodrich, and T. Idema, Physical Review E **91**, 032706 (2015).

[4] C. Huepe, G. Zschaler, A.-L. Do, and T. Gross, New Journal of Physics (2011).

[5] Rotating fish, `https://cwallpapersinaja.blogspot.com/2019/01/fish-shoal-wallpapers.html`, [Online, accessed July 6, 2019].

[6] migrating grasshoppers, `https://www.weforum.org/agenda/2015/11/how-can-we-control-locust-swarms/`, [Online, accessed 6 July, 2019].

[7] Jammed penguins, `https://physicsworld.com/a/huddling-emperor-penguins-undergo-phase-transition/`, [Online, accessed 6 July, 2019].

[8] L. D. Landau and E. M. Lifshitz, *Fluid mechanics* (Butterworth-Heinemann, Oxford, 1987).

[9] D. R. McCusker, Master's thesis, TU Delft, 2018.

[10] L. Verlet, Physical review **159**, 98 (1967).

[11] A. Rosato, K. J. Strandburg, F. Prinz, and R. H. Swendsen, Physical Review Letters **58**, 1038 (1987).

[12] T. Pöschel and H. J. Herrmann, EPL (Europhysics Letters) **29**, 123 (1995).

[13] J. Goodman, Stochastic differential equations, `https://www.math.nyu.edu/faculty/goodman/teaching/StochCalc2012/notes/Week9.pdf`, 2012.